View metadata, citation and similar papers at core.ac.uk

brought to you by CORE

provided by CERN Document Server

EUROPEAN ORGANIZATION FOR NUCLEAR RESEARCH
European Laboratory for Particle Physics

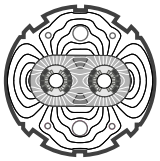

Large Hadron Collider Project

LHC Project Report 54

Experimental Evidence of Boundary Induced Coupling Currents in LHC Prototypes

L. Bottura, L. Walckiers and Z. Ang

Abstract

The field quality of 10 m long LHC dipole models has been measured with short rotating coils to explore its dependence on time and position. Multipoles exhibit a longitudinal periodic variation, with period equal to the twist pitch length. This periodicity is shown here to have at least two components with very different time constants. The amplitude of the component with the shorter time constant, in the range of 100 to 300 s, depends on position and time. Larger amplitudes are measured at early times after a ramp and close to regions with incomplete cable transposition with respect to the non-uniform external field change. As the multipoles periodicity is due to current imbalance in the cables, we attribute the short time scale variations to the presence of space and time decaying boundary induced coupling currents (*BICC's*) in the cable. An estimate of their value is given.

LHC Division

Paper presented at 1996 Applied Superconductivity Conference, Pittsburgh, Pa, August 25-30, 1996

Admnistrative Secretariat
LHC Division
CERN
CH - 1211 Geneva 23
Switzerland

18 September 1996

Experimental Evidence of Boundary Induced Coupling Currents in LHC Prototypes

L. Bottura, L. Walckiers and Z. Ang
CERN Division LHC, CH-1211 Geneva 23, Switzerland

Abstract—**The field quality of 10 m long LHC dipole models has been measured with short rotating coils to explore its dependence on time and position. Multipoles exhibit a longitudinal periodic variation, with period equal to the twist pitch length. This periodicity is shown here to have at least two components with very different time constants. The amplitude of the component with the shorter time constant, in the range of 100 to 300 s, depends on position and time. Larger amplitudes are measured at early times after a ramp and close to regions with incomplete cable transposition with respect to the non-uniform external field change. As the multipoles periodicity is due to current imbalance in the cables, we attribute the short time scale variations to the presence of space and time decaying boundary induced coupling currents (*BICC's*) in the cable. An estimate of their value is given.**

I. Introduction

Local field measurements in superconducting accelerator magnets have revealed a fine structure with longitudinal periodicity on all harmonic components [1-4]. The origin of this periodic variation, with a period identical to the inner layer cable twist pitch, is attributed to current distribution imbalance within the cable [5-10]. Such periodicity has already been measured on long models of the Large Hadron Collider (LHC) dipoles [4]. However, no systematic measurement has ever been performed in full-scale magnets to explore the dependence of the periodicity on longitudinal position and time. We present here a series of such measurements on two 10 m long LHC model dipoles.

The main motivation for this work is the idea that the strand magnetization can be affected by internal field changes in the cable associated to the current redistribution, a phenomenon visible when the transport current is constant [5,11]. This effect causes a drift of the field in the magnet at constant operating current, and must be known and corrected for accelerator operation especially during the particle injection phases and the initial stage of the energy ramp. We propose an interpretation of the current redistribution in the cable based on the model of Refs. [7,8], and an estimate of the current change in the strands which can be used to evaluate the internal field change in the cable.

II. Experimental set-up and Procedure

TABLE I
Geometric and Electric Parameters of the Inner Layer Cables

Magnet		MTP1A3	MTP1N2
Strand material		NbTi	NbTi
Strand diameter d	(mm)	1.3	1.3
Cable twist pitch Lp	(mm)	119	113
Cable width w	(mm)	17	17
Number of strands N		26	26
Average cross-contact resistance R_c	(μΩ)	14	7

Manuscript received August 25, 1996.

We have measured extensively two 10 m long models of the main LHC bending dipoles, conventionally named MTP1A3 and MTP1N2. These magnets achieve a field of 8.65 T at 12.8 kA operating current. The main characteristic of the cables used to wind the magnets are given in Table I (the inner-layer cables parameters are reported, as they are the one that mostly influence the field periodicity in the bore).

We will refer in the discussion to the harmonic components A_n and B_n of the 2-D complex expansion of the field **B** in the magnet cross section, defined as:

$$\mathbf{B}_y + i\mathbf{B}_x = \sum_{n=1}^{\infty}(B_n + iA_n)\left(\frac{z}{R_{ref}}\right)^{n-1} . \quad (1)$$

According to the definition (1) the harmonic components are expressed at the LHC reference position R_{ref}=10 mm. Because of its relevance for the machine operation, we will quote here results for the first allowed harmonics, normal sextupole B_3 and decapole B_5.

The field was measured along the bore of the magnets using two rotating coil units: a single 30 mm long coil and an array of 7x25 mm long adjacent coils. To achieve a periodic state in the current distribution we have cycled the magnet continuously at a given ramp-rate between low (550 to 890 A) and high current (10 to 13 kA) with a trapezoidal current waveform, checking that the field periodic pattern is reproducible from one cycle to the following. With the single coil the measurements taken at successive cycles and adjacent positions had to be synchronised to reconstruct the periodic pattern. The array of 7 coils covers a length of 175 mm, longer than a twist-pitch (of the order of 110 to 120 mm for the cables used), so that it was possible to derive directly the periodic pattern amplitude on all harmonics from a fit of points measured simultaneously.

Measurements were performed throughout the powering cycles at different ramp-rates, in the range of 10 A/s to 50 A/s, and at different positions along the magnet bore. The positions were chosen in particular so that they were close to the magnet ends and in the center. The center of the magnet straight section is the reference of the coordinate system. The typical time interval between single measurements at one position was 30 seconds. For all measurements we have set a relative time zero at the end of ramp down (start of the low current plateau). We refer here only to this relative time.

III. Results of Measurements

A. Field periodicity

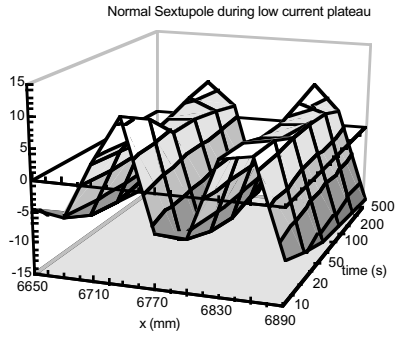

Fig. 1. Measurement of B3 periodicity during the low current (550 A) plateau after ramp-down at 50 A/s in the MTP1A3 model.

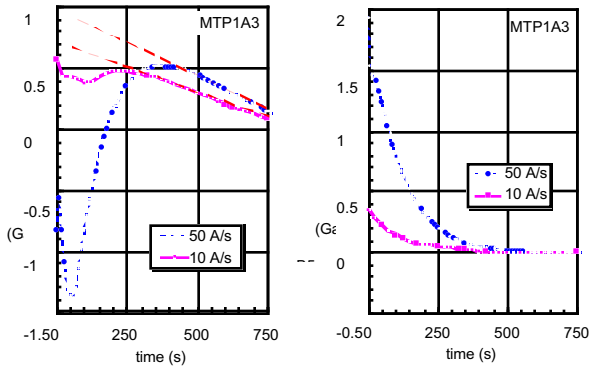

Fig. 2. Evolution of the amplitude of periodic pattern in normal sextupole and decapole during the low current (550 A) plateau after ramp-down, at two different ramp-rates in the MTP1A3 model.

We have reported in Fig. 1 a typical example of the the normal sextupole B3 periodicity along the length of the LHC dipoles, measured in MTP1A3 with the single coil during the low current plateau (550 A), following the ramp-down from high current (12.8 kA) at 50 A/s. The peak-to-peak amplitude of the B3 periodicity is of the order of 15 Gauss @ 10 mm. Similar measurements performed on the MTP1N2 model have given amplitudes in the range of 1 to 2 Gauss @ 10 mm. In spite of the fact that the two magnets are nominally identical, the powering history was similar, and the measured average interstrand contact resistance is comparable (R_c is in the range of 7 to 14 μΩ, see Tab. 1) the amplitude of the periodic pattern has nearly an order of magnitude difference in the two magnets. Note finally that the periodic variation is large with respect to the average value of B3, which in the case presented in Fig. 1 is of the order of 2 Gauss @ 10 mm. This implies that for magnetic measurements of average harmonics at low field a compensation of this effect will be needed.

B. Decay of the amplitude of the periodic pattern

From measurements of the type presented in Fig. 1 we have determined the time dependence of the amplitude during the low current plateau. Fig. 2 shows the decay of the B3 and B5 periodic pattern amplitudes in the MTP1A3 model during the low current plateau following the ramp-down at two ramp-rates, 10 and 50 A/s. The B3 amplitude decay exhibits two phases. After some fast initial change (till approximately 100 s) the amplitude decays in the first phase with a time constant of about120 s. After 300 to 400 s, depending on the ramp-rate used to approach the low current plateau, the decay leads to a slower drift with much longer time constant (dashed lines). The decay of the first phase is with good approximation proportional to the ramp-rate, while in the second phase the slope of the slow drift is only weakly dependent on the previous ramp-rate (about 30 % variation).

The decay of the B5 periodic pattern amplitude shows a clear first phase. The decay has the same time constant of 120 s as found on the B3 amplitude, and is proportional to the ramp-rate. However, no long-term drift is observed after the first phase. Similar results have been obtained in the MTP1N2 model, which showed however longer time constants in the range of 300 to 400 s.

C. Dependence on the longitudinal position

The dependence of the periodic pattern on longitudinal position has been obtained during successive cycles at the same ramp-rate, measuring a complete current cycle at each position. In Fig. 3 we plot the B3 periodic pattern amplitude measured in the MTP1A3 model at several times during the low-current plateau, after ramp-down from high current at 50 A/s. The periodic pattern is stronger closer to the connection end (see the sketch at the top of the figures identifying the magnet ends and straight portion). Furthermore, also the *decay* of the periodic pattern amplitude is stronger approaching the end (see the change from t=0 to t=500 s). The periodicity amplitude evolves towards a *baseline* value which is approximately constant along the whole length and slowly changing in time, as stated in the previous section. This baseline value is comparable to the one that has been measured scanning the magnet bore at constant current conditions and waiting a long time (more than 1000 s) after ramping before the scan.

Similarly, for the MTP1N2 model, in Fig. 4, a larger periodic pattern and decay is found approaching the magnet ends. The pattern is broadly symmetric with respect to the magnet center (note that the measuring points are not placed exactly symmetrically - those on the connection side of the cold mass cover the coil ends while on the non-connection

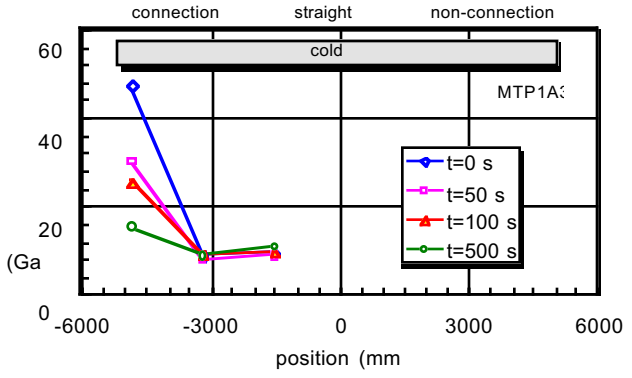

Fig. 3. Amplitude of periodic pattern of normal sextupole B3 during the low current (550 A) plateau at different times after ramp-down, at 50 A/s. Measurements at different locations along the length of the MTP1A3 dipole magnet.

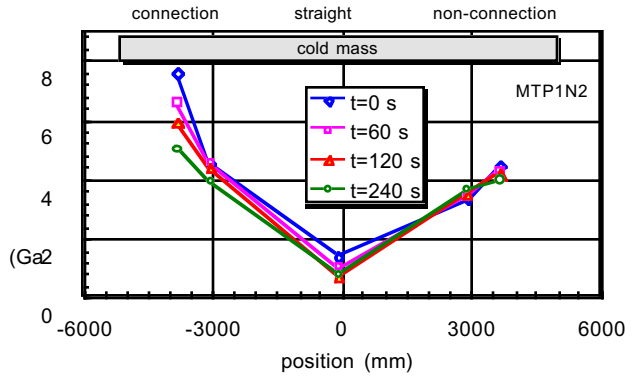

Fig. 4. Amplitude of periodic pattern of normal sextupole B3 during the low current (890 A) plateau at different times after ramp-down at 20 A/s. Measurements at different locations along the length of the MTP1N2 dipole magnet (the sketch identifies their location with respect to the winding).

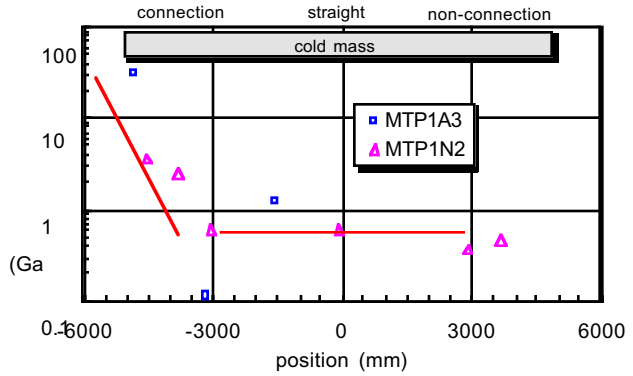

Fig. 5. Change of the amplitude of periodic pattern of normal sextupole during the low current (550 A) plateau after ramp-down at 50 A/s for the MTP1A3 dipole and at 20 A/s for the MTP1N2 dipole. The solid lines are added to guide the eye.

side they do not). Comparing Figs. 3 and 4 we finally observe the difference in the pattern amplitude, which is much larger in MTP1A3 than in MTP1N2, as stated earlier.

To put the end effect into evidence we have plotted in Fig. 5 the *change* of periodic pattern amplitude between the start and the end of the low current plateau, as obtained from the data plotted in Figs. 3 and 4. We have superposed the results of the two magnets, although the two ramp-rates are different. This operation has removed the large difference in the baseline values, and evidences the sharp rise in the amplitude decay approaching the connection end, showing also that the changes observed in the straight part are small (note the log-scaling on the plot). Although the number of measurement points does not allow a precise determination of the characteristic length of the end effects, the impression is that this length must be of the order of 1 to 2 m.

IV. Discussion

Several sources can be identified as potentially responsible for current imbalance in a cable:

1. non-uniform contact resistance at the cable joints;
2. non-uniform critical current density J_c at high field[10];
3. incomplete cable transposition with respect to self and external field change [7-9]. In accordance with the nomenclature of [8] we call the resulting circulating currents *boundary induced coupling currents* (BICC's);
4. non-uniform cable cross-contact resistance R_c along the length of the cable[6]

The first two mechanisms result in a current redistribution process along the cable analog to a current diffusion process with very long time constants up to steady-state [10]. Both are critical with respect to parameters that are very difficult to control in the magnet. The result is that both effects can produce very different current distributions in similar magnets. Owing to the long time constants both will show strong dependence on the long term powering history.

The third and fourth, on the other hand, depend on the winding geometry and cable uniformity. It can be shown [8] that the characteristic times (needed to *fill* the winding with a current imbalance) associated with both are smaller than those of the current distribution induced by the joint resistance and critical current differences.

We recall from our measurements that two very different time scales have been identified in the variation of the pattern amplitude. Similar amplitude decays were observed on the fast (100 to 400 s) time scale, in contrast with a large difference between MTP1A3 and MTP1N2 on the slow time scale. We propose therefore to associate the long term variations to joint resistance and critical current differences, and the short term changes to net flux linkage and non-uniform R_c.

In a dipole accelerator magnet, the main source of transposition errors is in the coil ends, where the cable is bent and the field variation along the cable is such that a net flux linkage can result [7,8]. This error appears every half turn, *i.e.* approximately 10 m in the LHC long models tested so far. Because of the periodicity with the turn length, the observer scanning the bore of the magnet sees the turn *end-effects* as symmetric with respect to the magnet center (two equal sources are located at each coil end). On the other hand, the current distribution from the joints, or due to non-uniform J_c, should eventually appear as uniform along the bore (no symmetry). The measurements have shown that approaching the connection end of the coil the pattern amplitude after ramping is indeed larger, and has a stronger decay on the fast time scale (we have no measured points in the non-connection end to justify a stronger statement on the decay symmetry).

Because of the argument on time scales and based on the reasoning on the space distribution, we associate the fast decaying component of the field periodic pattern with the presence of cable BICC's driven by the flux linkage in the coil ends. For both MTP1A3 and MTP1N2 the currents induced by non-uniform R_c seem to play a minor role.

In the case of uniform R_c the following approximations for the BICC's decay time τ, diffusion length ξ, and maximum induced strand current ΔI in a Rutherford cable have been derived in [8]:

$$\tau \approx 1.2 \cdot 10^{-8} \frac{N \pi d^2}{\rho}. \qquad (2)$$

$$\xi \approx 0.5\sqrt{\frac{R_c L_p \pi d^2}{2\rho N}} \tag{3}$$

$$\Delta I \approx 0.88 \frac{w\xi}{R_c}\left(1 - e^{-\frac{N}{96}}\right)\Delta\dot{B} \tag{4}$$

where L_p is the cable twist pitch, d the strand diameter, N the number of strands in the cable, w is the cable width and $\Delta\dot{B}$ is the *variation* of field change rate along the cable length causing the net flux linkage. Finally, ρ is an effective strand resistivity that is used in the model to represent the longitudinal electric field associated to current flow in or out of the superconducting filaments.

Based on the results from our measurements, we can try to verify these scalings. Firstly we take the characteristic times τ as measured from the local amplitude decays. From these, and from (2) we can determine the value of the effective longitudinal resistivity ρ. We obtain values of 1.1×10^{-14} Ωm and 4.7×10^{-15} Ωm for MTP1A3 and MTP1N2 respectively. With these values we can use (3) to estimate the characteristic length ξ. In both cases we have values of the order of 1.5 to 2 m (the lower longitudinal resistivity in MTP1N2 is balanced by a lower cross contact resistance in the cable, as reported in Table I). These values are coherent with the observed longitudinal envelope of the amplitudes profile (see Fig. 5), and thus prove the internal consistency of the model.

We can try now to estimate the current imbalance in the strands from (4), and from the results above. At 50 A/s ramp-rate, one of the measured points in MTP1A3, the maximum field change rate on the cable in the straight section is 35 mT/s. This value drops nearly to zero in the coil ends. Therefore we can take that the variation of the field change rate along the length is $\Delta\dot{B} \approx 35$ mT/s. The maximum current induced in a single strand is then of the order of 70 A in the MTP1A3 model and 140 A in the MTP1N2 model.

To verify this estimate, we have used the field measurements in the magnet ends of MTP1A3 taken after a 50 A/s ramp-down from high field to compute in a different way the current imbalance in the cable. We have modelled the inner layer winding as two thin current sheets concentric with the magnet bore. In each sheet a harmonic current distribution with two components was assumed: a first component with the same value and sign in both sheets, responsible for the average of the field harmonics, and a second component with equal value but opposite sign, periodic along the magnet, to model the periodic pattern originated by the current imbalance. The current distributions in both sheets were then obtained analytically from the measured field harmonics. Depending on the assumptions made on the cable current distribution (mainly on the location of the current sheets within the cable), we have obtained current imbalances that are in the range of 15 to 75 A, in fair agreement with the predictions of the model.

V. CONCLUSIONS

Measurements of local field along the bore of two full-scale models of the LHC dipoles have shown that the longitudinal field periodicity shows two clear time scales. The faster one, in the range of 100 to 300 s can be attributed to boundary-induced coupling currents (BICC's) and shows some reproducibility in similar magnets. On the slower time scale (larger than 1000 s) the field periodicity has large scattering within magnets.

We have verified the time constant, diffusion length and inferred current imbalances against the predictions of a model [7,8] describing the BICC's and found reasonable agreement. We believe therefore that at least one component of the field periodicity can be explained.

REFERENCES

[1] H. Brueck, et al., Observation of a Periodic Pattern in the Persistent Current Fields of the Superconducting HERA Dipole Magnets, Proc. of 1991 Part. Acc. Conf, San Francisco, 1991

[2] A.K. Gosh, K.E. Robins, W.B. Sampson, The Ramp Rate Dependence of the Sextupole Field in Superconducting Dipoles, IEEE Trans. Mag., **30**, 4, 1718-1721, 1994.

[3] W.B. Sampson, A.K. Gosh, Induced Axial Oscillations in Superconducting Dipole Windings, IEEE Trans. Appl. Sup., **5**, 2, 1036-1039, 1995.

[4] J. Buckley, et al., Dynamic Magnetic Measurements of Superconducting Magnets for the LHC, IEEE Trans. Appl. Sup., **5**, 2, 1024-1027, 1995.

[5] R. Stiening, A Possible Mechanism for Enhanced Persistent Current Sextupole Decay in SSC Dipoles, SSCL-359, 1991, unpublished.

[6] A.A. Akhmetov, A. Devred, T. Ogitsu, Periodicity of Crossover Currents in a Rutherford-type Cable Subjected to a Time Dependent Magnetic Field, Jour. Appl. Phys., **75**, 6, 3176-3183, 1994.

[7] A.P.Verweij, H.H.J. ten Kate, Super Coupling Currents in Rutherford Type of Cables due to Longitudinal Non-homogeneities of dB/dt, IEEE Trans. Appl. Sup., **5**, 2, 404-407, 1995.

[8] A.P.Verweij, Electrodynamics of Superconducting Cables in Accelerator Magnets, Ph.D., Twente University (NL), 1995.

[9] L. Krempansky, C. Schmidt, Influence of a Longitudinal Variation of dB/dt on the Magnetic Field Distribution of Superconducting Accelerator Magnets, Appl. Phys. Lett., **66**, 12, 1545-1547, 1995.

[10] A.Akhmetov, A.Devred, R.Mints, R.Schermer, Current Loop Decay in Rutherfor Type Cables, Supercollider, **5**, 443-446,1993

[11] L. Bottura, L. Walckiers, R. Wolf, Field Errors Decay and "Snap-Back" in LHC Model Dipoles, Presented at 1996 Appl. Sup. Conf, Pittsburgh, unpublished.